[9] Excitonic optical nonlinearity of dielectric nanocomposites in weak optical fields

D.V. Storozhenko[1], V.P. Dzyuba[1], Y.N. Kulchin[1,2], A.V. Amosov[1]
[1] Institute of Automation and Control Processes, FEB Russian Academy of Sciences, Vladivostok, Russia,
[2] Far Eastern Federal University, Vladivostok, Russia

Abstract

The paper presents a model of optical nonlinearity in a dielectric nanocomposite for wavelengths ranging from 200 to 800 nm and intensities of up to 1000 W/cm^2. Results of the numerical modeling of the optical response in a nanocomposite consisting of dielectric nanoparticles Al_2O_3 with low volume concentration (of the order of 0.3 %) embedded in a transparent dielectric liquid matrix are presented. It is found that with the volume concentration remaining unchanged, the value of nonlinear response in unit volume increases with decreasing nanoparticles size. The spectrum of the nonlinear extra term of the refraction index is shown to be affected by various parameters, such as the size and anisotropy of nanoparticles. It is notable that for 45-nm Al_2O_3 nanoparticles with 0.3% volume concentration the value of the nonlinear optical response reaches $1.5 \cdot 10^{-4}$ cm^2/W near the resonant absorption band.

Keywords: *exciton; optical nonlinearity; dielectric composites; optical spectrums; nanoparticles; refraction index; resonant susceptibility.*

Citation: *Storozhenko DV, Dzyuba VP, Kulchin YN, Amosov AV. Excitonic optical nonlinearity of dielectric nanocomposites in weak optical fields. Computer Optics 2016; 40(6): 855-862. DOI: 10.18287/2412-6179-2016-40-6-855-862.*

Introduction

Unique optical properties of dielectric nanocomposite materials have been discussed a lot during the last decade. Particular attention is given to those features that are poorly worked out or completely missing in dielectrics with high volume concentration. For example, additional effects of the medium, external field, size, and shape of nanoparticles influenced on dielectric transmittance and luminescence spectra have been determined [1 – 3]. The similar impact of the medium is also observed in semiconductor nanoparticles [4 – 6]. In papers [7 – 10], the non-linear optical response has been detected in some dielectric nanocomposite materials for intensities ranging of up to 1 kW/cm^2, i.e. it is insufficient to launch multiphoton processes, photoionization or any other nonlinear processes. In papers [11, 12], the authors come to the conclusion, discussing nature of such type of nonlinearity, that the reason thereof is the key influence of exitonic levels in dielectric nanoparticles on the general transmission spectrum. The authors of paper [13] define conditions favorable for long-lived excitonic states occurred in dielectric nanoparticle materials embedded in a transparent dielectric liquid matrix with linear optical properties within the optical range. Experimental results for these materials published in papers [14 – 19] have shown that when radiation intensity was about 150 – 250 W/cm^2, the nonlinear extra term of the refraction index was $n_n = 10^{-4} \div 10^{-5}$ near the resonant absorption band. These findings correlate very accurately with a theoretical model of such nonlinearity proposed in paper [20]. However, it is necessary to analyze the influence of the size, shape, and concentration of nanoparticles in order to forecast optical properties of nanocomposite dielectric materials. Numerical methods for solving Schrodinger equations are used in theoretical research of optical nonlinearity, for example, in papers [21, 22]. It is extremely difficult to use this approach for nanosystems consisting of thousands of interacting elements even for numerical solution, since the increasing number of interacting elements considerably complicates a form of an equation. A possible solution of the problem may consist in entering into the equation those functions, which describe behavior effects of some system parameters based on the existing empirical data. This approach requires a mathematical model of physical processes that is correlated with experimental data. In previous papers [9, 13, 14, 17 – 20], the approximation of the excitonic optical response was made at different parameters ob-

tained empirically for each particular case. The purpose of this paper is to develop representation of a model by considering new conditions for defining parameters taken from experiments conducted earlier.

1. Resonant absorption model

By dielectric nanocomposites we mean dielectric nanoparticles embedded in a transparent dielectric liquid matrix with linear optical properties within a visible range. Papers [14, 17 – 20] describe such nanocomposites with wide excitonic absorption bands, lying within a band gap, available in absorption and luminescence bands. Pronounced peaks of the excitonic absorption are generally observed in semiconductors at low temperatures (up to tens of K) [23, 24]. The excitonic absorption bands can be also observed in dielectric nanocomposites at a temperature of about 300 K. This appears when the Louis de Broglie wavelength of the exciton is compared to the size of a nanoparticle. In this case, the effect of the nanoparticle-matrix interface is shown as increasing depth of a potential well where the exciton is located (an electron and a hole) and it results in increasing the hole-electron binding energy. In classical understanding, this means that a negatively charged layer occurs inside the interface that prevents destruction of exciton coherence. This happens when the dielectric constant of the nanoparticle material is greater than the dielectric constant of the surrounding matrix. As a result, exciton absorption lines move depthward to the band gap and become apparent in the visible range of the absorption bands, in spite of the high (> 6 electron volt) band gap energy [19]. Nanoparticle and surrounding matrix materials must be selected not only by evaluating the dielectric constant on the optical frequency, but also in line with transparency in order to reduce the heat effect. This also requires low volume concentration. High concentration of nanoparticles at which the particles start to interact with each other is undesirable as this will reduce the value of the nonlinear optical response. Therefore, we have analyzed the case with low volume concentration (of the order of 0.3 %) that allows us to neglect the mutual influence in nanoparticles and to fulfill a condition of optical transparency of nanocomposites. Probability of two-photon processes is insignificant in weak optical fields, so we can assume that in quantum concepts the nanoparticles are represented as a set of independent two-level systems distributed with volume density and interacting with the medium independently from each other [25]. The nonlinear optical response of the medium is proportional in this model to the complex susceptibility per unit volume considering that the full susceptibility of material $\tilde{\chi}$ with intensities ranging of up to 1000 W/cm^2 is represented by a sum of linear and nonlinear excitonic susceptibilities.

$$\tilde{\chi} = \tilde{\chi}_0 + \tilde{\chi}_R . \quad (1)$$

The process of exciton creation is resonant in its nature at certain frequencies. Therefore, we must use a model of complex resonant susceptibility with population-level differences [26]:

$$\tilde{\chi}_R = \frac{Np^2 \ddot{A}\rho_{ng}(\omega, I)}{\hbar} \cdot \frac{(\omega - \omega_0) + i\Gamma}{(\omega - \omega_0)^2 + \Gamma^2}, \quad (2)$$

$$\Delta\rho_{ng}(\omega, I) = \Delta\rho^0 \left[1 - \frac{I / I_s}{(\omega - \omega_0)^2 + \Gamma^2 (1 + I / I_s)} \right], \quad (3)$$

where $\tilde{\chi}_0$ is a linear part of susceptibility of materials, $\tilde{\chi}_R$ is the resonant non-linear extra term of susceptibility of materials, ω_0 is the resonance frequency, Γ is an absorption line half-width, ħ is the Plank constant ("h-bar"), N is a number of charge carriers in optical distance ranging, Drng is the population-level difference of energies of states | n ⟩ and | g ⟩, p = ⟨ n | e · r$_i$ | g ⟩ is a projection of the net electric dipole moment of electron transition in the nanoparticle from state ⟨ n | to state | g ⟩ towards the polarization direction of the external optical radiation, $\Delta\rho_0$ is the equilibrium heat population difference with no external fields, and Is is the level of saturation of a two-level system at which a half of charge carriers have passed to the excited state. Note that a priori dipole moment of the nanoparticle is unknown. However, in classical understanding, we can interpret exciton excitation as charge redistribution in the nanoparticle and creation of the average dipole moment d_{exc} in such a way that the dipole moment becomes proportional to p_0 ~ a×e. In this case, it seems obvious that the value of this dipole moment will depend on the size and shape of the nanoparticle. The induced dipole moment d_{exc} in the nanoparticle, in case of isotropic nanoparticle material, may coincide with the electric-field vector E, whereas in case of anisotropic material, the net dipole moment of the nanoparticle may be inconsistent with E. In this case, there occurs a torque, which will try to turn the nanoparcle along the vector E. This would result in increasing polarization in unit volume. Note that anisotropy of nanoparticles may occur in the process of polarization not only because of material properties, but also because of the nanoparticle shape. The torque of nanoparticle orientation will be proportional to the intensity of the external field. The parameter of nanoparticle orientation along the field will be a complex function of the intensity I that is included therein through the dipole moment and the external-field interacting force. It seems to be impossible to write down analytically a formula for this dependence. However, it would be fair to introduce the

orientation factor A(I), which simulates the dipole moment square behavior while changing the radiation intensity:

$$p^2 = p_0^2 A(\mathrm{I}). \quad (4)$$

Dependence of the orientation factor from the intensity I is defined in this paper as follows:

$$A(I) = 1 - \mathrm{e}^{-I/\alpha}. \quad (5)$$

The shape of nanoparticles is determined in the model using the orientation factor of the nanoparticle polarization vector along the vector of the electric field intensity that depends on the intensity of polarized radiation. The factor α sets the susceptibility to radiation intensity and is determined by the shape of nanoparticles or, more precisely, by the difference of characteristic dimensions along the basis vectors. In other words, the value of this factor is proportional to anisomery of nanoparticles that was experimentally studied in previous research. The issue of exact calculation or analytical representation of this factor, using distribution of sizes and shapes of nanoparticles in volume of metamaterial with a liquid matrix, is still open. Therefore, this factor is considered to be a specified parameter in this model, and $\alpha \to 0$ for a spherical shape of the nanoparticle with the isotropic dielectric constant tensor.

2. Description of modeling parameters

After having transformed the above equations (3 – 5), we write over the expression for the resonant non-linear extra term of the exciton susceptibility as follows:

$$\tilde{\chi}_R = \frac{NA(\mathrm{I})p_0^2\Delta\rho^0}{\hbar} \cdot \frac{(\omega-\omega_0)+i\Gamma}{(\omega-\omega_0)^2+\Gamma^2(1+I/I_s)}. \quad (6)$$

The right fraction in the formula (6) represents a Lorentsian model in saturation spectroscopy, in which when $I_s = const$, the real part is an uneven function, whereas the imaginary part is an even function. It is known that the susceptibility $\tilde{\chi}$ is related to the dielectric permittivity, and yet to the refraction index. Note that in this case the real part of the formula (6) sets the non-linear extra term of the refraction index, whereas its imaginary part gives the extra term to the material absorption coefficient. Let's write the expression for connecting the susceptibility $\tilde{\chi}_R$ with the complex refraction index for dielectric nanoparticles in a solution as follows:

$$\tilde{n}(\omega,\mathrm{I}) = \tilde{n}_0 + \tilde{n}_n(\omega,\mathrm{I}) = n_0 + (2\pi\tilde{\chi}_R(\omega,\mathrm{I}))/n_0. \quad (7)$$

For numerical simulation, it is necessary to enumerate all input parameters and define the range of their values.

- $\Delta\rho_0 \in [0, 1]$ is the equilibrium heat population difference. This model considers the case with a stationary temperature of 300 K; that's why we can believe that $\Delta\rho_0 = const$;
- $a \in [5, 100]$ nm is a specified size of a dielectric nanoparticle. We analyzed this particular range of the nanoparticle sizes;
- $N \in [10^{12}, 10^{15}]$ in cm^{-3} is the number of charge carriers in unit volume. In this model, it is taken to be equal to the number of nanoparticles and is calculated via material volume concentration and nanoparticle volume at a specified value of a. We analyzed the case with volume concentration of the order of $f = 0.3$ %;
- $p_0 = a \times e$ is the maximum dipole moment of the nanoparticle, where a is the size of the nanoparticle and the charge of the electron e is set in CGS system;

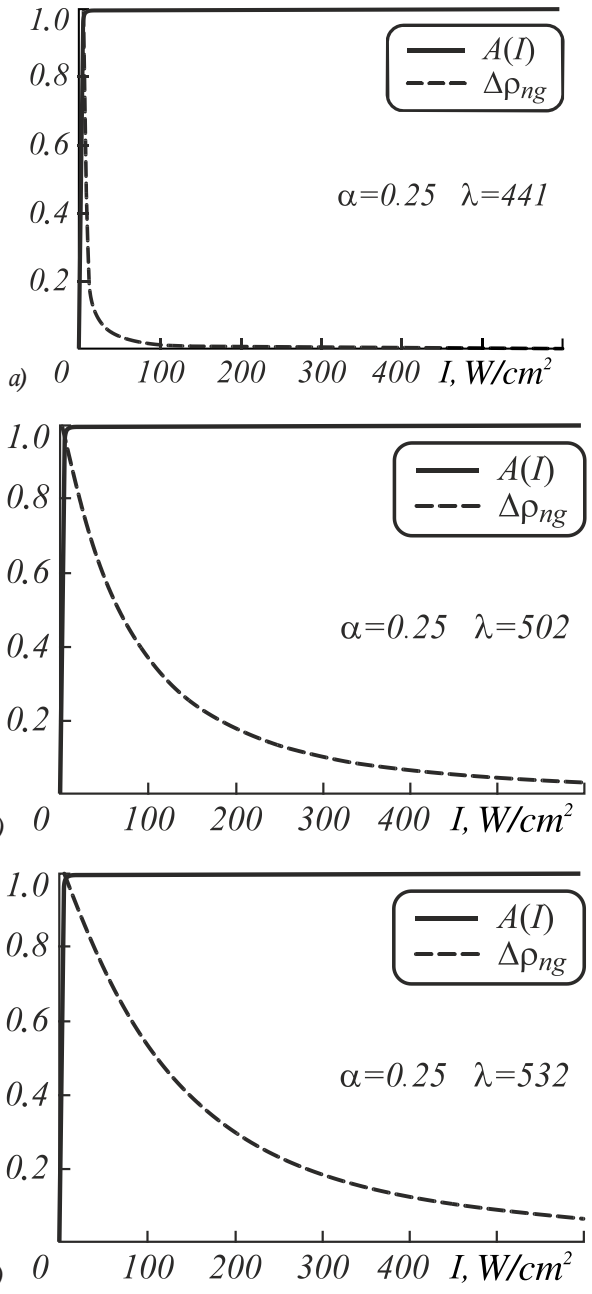

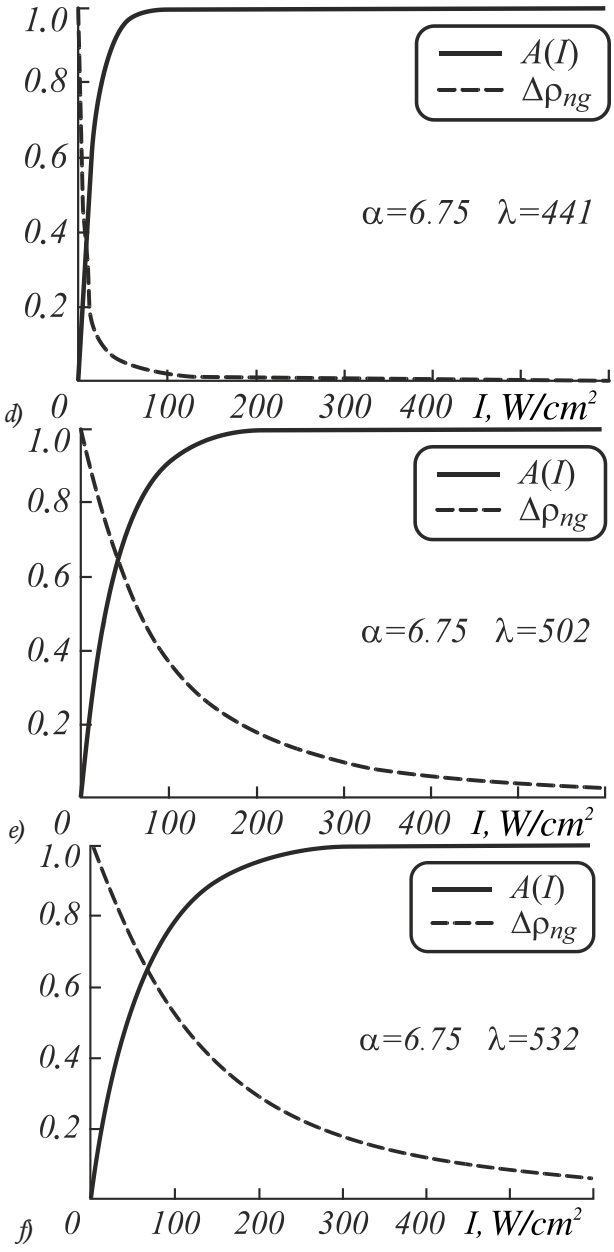

Fig. 1. Graphs of two competitive processes: the level-population difference $\Delta\rho_{ng}$ and the orientation factor A(I). Dependence on the intensity at different fixed values of α and λ. This behavior corresponds to spherical (a, b, c) and non-spherical (d, e, f) shapes of nanoparticles

ω_0, and Γ are the resonant frequency and the absorption line half-width, respectively. They may be specified based on experimental data. For convenience, our model shows them in dimensions of the wavelengths λ_0 and Γ_λ (in nm) corresponding thereto;

ν_0 is the refraction index of high-volume material of dielectric nanoparticles on the optical frequency (specified for reference only);

$\alpha \in [1, 100]$ is the anisomery coefficient for the nanioparticle; in case of the isotropic dielectric constant tensor and the spherical shape of nanoparticles, $\alpha \to 0$. Increasing values of the coefficient means that one of its basis vectors excels the others;

$I_\sigma \in [20, 200]$ W / cm^2 means threshold saturation at which a half of free charge carriers are induced. It is specified based on experimental data.

The non-linear susceptibility response may be easily considered as the product of two competitive processes: the orientation factor $A(I)$ and the level population difference $\Delta\rho_{ng}$, whose graphs are given in Fig. 1. These processes are to be calculated in order to select the most appropriate working area in practical application of exciton nonlinearity of dielectric nanocomposites, for example, in optical switches [27 – 29]. When analyzing the above expression (7), we may notice that the susceptibility value $\tilde{\chi}_R$ is proportional to N and p_0^2, which, in their turn, are specified with the volume concentration f and the size of nanoparticles a.

When f = const, while increasing the size of nanoparticles, N is reduced proportionally to a^3, whereas p_0^2 is increased proportionally to a^2. This brings us to the conclusion that decreasing the particles sizes would result in increasing the non-linear optical response at the same volume concentration. As may be inferred from the above equations (3 – 5), the non-linear part of the susceptibility $\tilde{\chi}_R$ changes, depending on the frequency and intensity.

3. Modeling results

Using the non-linear susceptibility and well-known models for calculating the refraction index of the two-composite medium, for example, a Maxwell Garnett model, it is possible to build transmission, absorption and material scattering spectra. We can find expressions for calculation of scattering cross-section spectra and material absorption spectra in paper [26]. However, because of predominance of contribution of a linear component over a nonlinear one in several orders, it is reasonable to show proper individual spectra, corresponding only to the non-linear extra term of the complex refraction index.

To simulate experimental data [18] with dielectric nanoparticles Al_2O_3 dissolved in transparent oil, the following values of parameters are entered into the model: $\Delta\rho^0 = 0.9$, a = 45 nm, $n_0 = 1.65$, $\lambda_0 = 437$ nm, $\Gamma_\lambda = 27.4$ nm, f = 0.3 %, $I_s = 50$ W/cm^2, $\alpha = 3.5$. Figure 3 gives the graphs for the complex non-linear

extra term $\tilde{n}_n(\omega, I)$ amounting to $1.5 \cdot 10^{-4}$ cm^2/W (Fig. 2r). We consider the cases with the fixed wavelengths (Fig. 2a – c) or intensities (Fig. 2d – f).

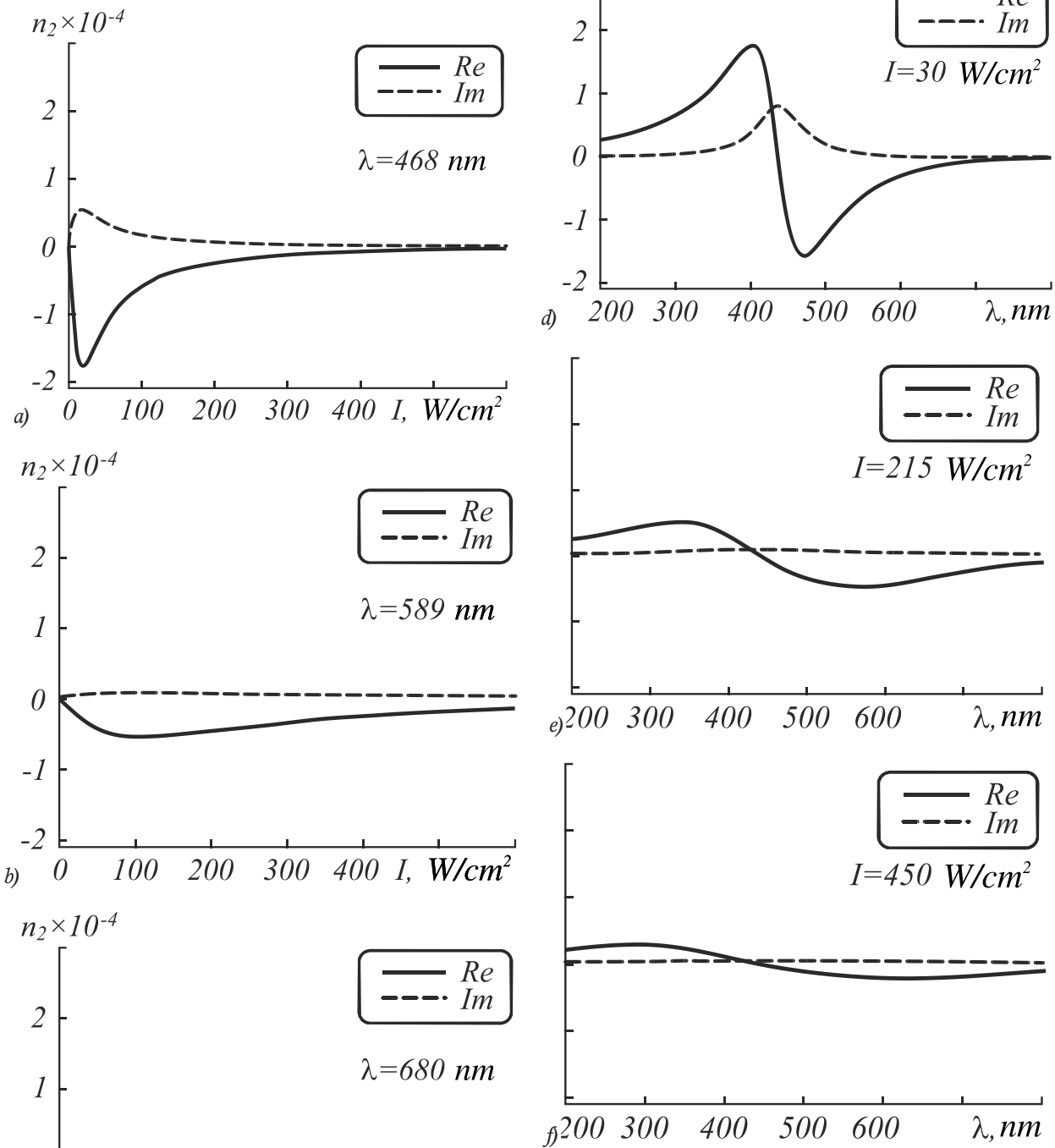

Fig. 2. Graphs of the non-linear extra term at fixed values of λ (a, b, c) and fixed intensities (d, e, f). The real and imaginary parts are given separately

Calculations of wavelength spectra show that while changing the intensity, the imaginary part of the non-linear extra term reduces faster than its real part. When passing through the resonant frequency λ_0, the real part

of the non-linear extra term $\tilde{n}_n(\omega, I)$ changes its sign. While changing the intensity (Fig. 2*d – f*), broadening of the real-and-imaginary-part band $\tilde{n}_n(\omega, I)$ can be observed thus decreasing the amplitude of the values. It can also be seen in Fig. 2*a – c* that while moving from the resonant frequency, a point of extremum is displaced in the intensity graphs of the real and imaginary parts. It can also be seen in Fig. 2*a, b* that with increasing intensity the non-linear response first is increasing, and then is decreasing. Such decrease of the value of the non-linear extra term, while increasing the intensity, may be explained by the influence of the process of saturation for the two-level model when the level-population difference is reduced. The real and imaginary parts of the non-linear extra term $\tilde{n}_n(\omega, I)$ may be easily estimated in the shape of three-dimensional allocation maps of intensities and wavelengths (Fig. 3*a, b*).

Allocation of the real part of the refraction index can be clearly seen from the image analysis at different wavelengths and intensities. At a relatively small absorption line half-width, the area of changing the non-linear extra term of the real part covers a large optical range. This means that the resonant absorption band available in the violet part of the spectrum, being the exciton in nature, may be used at a considerable distance (up to 200 nm) therefrom towards the red area.

Conclusion

Behavior effects of the excitonic non-linear optical response have been demonstrated, depending on the intensity of the external monochromatic radiation. The peculiar feature is that when the radiation intensity increases gradually, the response first increases and then decreases.

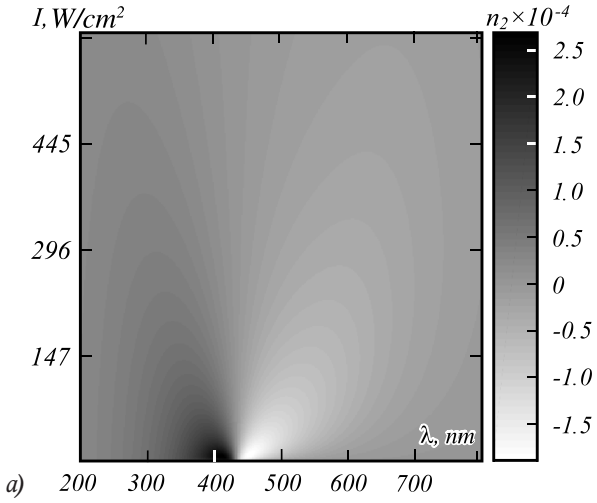

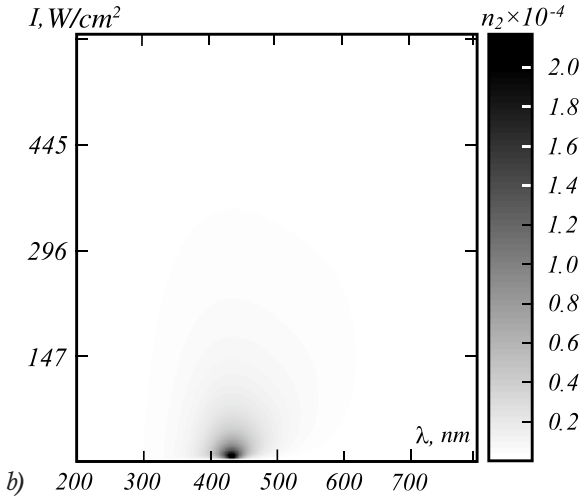

Fig. 3. The real (a) and imaginary (b) parts of the non-linear extra term n2. The two-dimensional allocation map for values of the non-linear extra term depending on the intensity and wavelength of polarized radiation

Such behavior of the excitonic nonlinearity in dielectric nancomposites differentiates it from the known quadratic and cubic nonlinearity of material. The value of the non-linear extra term of the refraction index is up to $1.5 \cdot 10^{-4}$ with low volume concentration (of the order of 0.3 %) and rather low intensities of up to 1000 W/cm^2. It is practically feasible to be used in optical devices, for example, in optotransistors (transphasors) [30]. The represented model of numerical calculations allows us to analyze the excitonic optical nonlinearity at different frequencies and to keep track of behavior of the complex extra term $\tilde{n}_n(\omega, I)$ at different sizes of particles and some other parameters. For example, as follows from the numerical modeling, it is found that the value of the non-linear optical response $\tilde{\chi}_R$ is proportional to the size of nanoparticles and their quantity in unit volume *N*. With the volume concentration of nanoparticles remaining unchanged, the value $\tilde{\chi}_R$ increases with decreasing nanoparticles size. So it is recommended to use less size particles to increase the non-linear optical response. It is found that the contribution to the non-linear optical response of the orientation factor $A(I)$ increases with increasing anisotropy of nanoparticles. It becomes the most apparent near the resonant frequency, whereas by removing therefrom, the contribution of the non-linear response decreases. Anisomery of nanoparticles also affects the non-linear optical response behavior depending on the intensity. When increasing a ratio of dimensional sides of particles, the orientation factor grows at a much slower rate with increasing intensities. It is notable that a be-

havior pattern of the non-linear optical response is meant to be an indicator of the particle sphericity with the isotropic polarizability tensor.

Acknowledgment

The work is partially funded by grants of the Fundamental Research Program of the Far Eastern Branch of the Russian Academy of Sciences (No. 0262-2015-0094, No. 0262-2015-0059).

References

1. Ganeev RA, Usmanov T. Nonlinear optical parameters of various media. Quantum Electronics 2007; 37(7): 605-622.

2. Kulchin YN, Dzyuba VP, Scherbakov AV. Light transmission spectrum of the dielectric nanoparticles inserted into a dielectric matrix. Semiconductors 2009; 43(3): 331-339. DOI: 10.1134/S1063782609030130.

3. Dzuba V, Kulchin Y, Milichko V. Effect of the shape of a nano-object on quantum-size states. Journal of nanoparticle research 2012; 14(11): 1208. DOI 10.1007/s11051-012-1208-7.

4. Divya S, Sebastian I, Nampoori VPN, Radhakrishnan P, Mujeeb A. Tailoring optical properties of TiO2 in silica glass for limiting applications. Chinese Physics B 2014; 23(3): 034210. DOI: 10.1088/1674-1056/23/3/034210.

5. Yan X-Y, Zhang K-X, Yao C-B, Li Q-H. Ultrafast nonlinear optical properties and optical Kerr effect of In-doped ZnO nanowires. Materials Letters 2016; 176: 49-51. DOI:10.1016/j.matlet.2016.04.058.

6. Sivasubramanian D, Ponnusamy R, Gandhiraj V. Low power optical limiting and thermal lensing in Mn doped ZnO nanoparticles. Material Chemistry and Physics 2015; 159: 93-100. DOI:10.1016/j.matchemphys.2015.03.056.

7. Koushki E, Farzaneh A, Majles Ara MH. Modeling absorption spectrum and saturation intensity of ZnO nano-colloid. Optik 2013; 125(1): 220-223. DOI:10.1016/j.ijleo.2013.06.007.

8. Kim HS, Lee MH, Jeong NC, Lee SM, Rhee BK, Yoon KB. Very high third-order nonlinear optical activities of intrazeolite PbS quantum dots very high third-order nonlinear optical activities of intrazeolite PbS. J Am Chem Soc 2006; 128(47): 4-6. DOI: 10.1021/ja0661966.

9. Dzuba VP, Krasnok AE, Kulchin YN. Nonlinear refractive index of dielectric nanocomposites in weak optical fields. Tech Phys Lett 2010; 36(11): 973-977. DOI: 10.1134/S1063785010110015.

10. Ganeev RA, Suzuki M, Baba M, Ichihara M, Kuroda H. Low- and high-order nonlinear optical properties of BaTiO3 and SrTiO3 nanoparticles. J Opt Soc Am B 2008; 25(3): 325-333. DOI: 10.1364/JOSAB.25.000325.

11. Dneprovskii V, Smirnov A, Kozlova M. Self-diffraction of ultrashort laser pulses under resonant excitation of excitons in a colloidal solution of CdSe/ZnS quantum dots. Quantum Electronics 2013; 43(10): 927-930.

12. Dneprovski VS, Zhukov EA, Kozlova MV, Wumaier T, Hieu DS, Artem'ev MV. Absorption saturation and self-action processes under resonant excitation of the basic exciton transition in CdSe/ZnS colloidal quantum dots. Physics of the Solid State 2010; 52(9): 1941-1946.

13. Dzuba V, Kulchin Y, Milichko V. Photonics of heterogeneous dielectric nanostructures. Ch 15. In Book: Ebrahimi, F, ed. Nanocomposites – New Trends and Developments. InTech; 2012. ISBN: 978-953-51-0762-0, DOI: 10.5772/50212.

14. Milichko VA, Nechaev AI, Valtsifer VA, Strelnikov VN, Kulchin YN, Dzyuba VP. Photo-induced electric polarizability of Fe3O4 nanoparticles in weak optical fields. Nanoscale Research Letters 2013; 8(1): 317. DOI: 10.1186/1556-276X-8-317.

15. Kupchak IM, Kruchenko YuV, Korbutyak DV. Exciton states and photoluminescence of Si and Ge nanocrystals in Al2O3 matrix. Semiconductors 2008; 42(10): 1194-1199. DOI: 10.1134/S1063782608100096.

16. He J, Ji W, Ma GH, Tang SH, Elim HI, Sun WX, Zhang ZH, Chin WS. Excitonic nonlinear absorption in CdS nanocrystals studied using Z-scan technique. J Appl Phys 2004; 95(11): 6381-6386. DOI: 10.1063/1.1711183.

17. Milichko V, Dzuba V, Kulchin Y. Unusual nonlinear optical properties of SiO2 nanocomposite in weak optical fields. Applied Physics A 2013; 111(1): 319-322. DOI 10.1007/s00339-013-7609-3.

18. Milichko VA, Dzyuba VP, Kulchin YN. Anomalous optical nonlinearity of dielectric nanodispersions. Quantum Electronics 2013; 43(6): 567-573. DOI:10.1070/QE2013v043n06ABEH015171.

19. Kulchin YN, Dzyuba VP, Milichko VA. Dielectric nano-systems with unique optical properties. Advanced Materials Research 2013; 677: 36-41. DOI:10.4028/www.scientific.net/AMR.677.36.

20. Dzyuba VP, Krasnok AE, Kulchin YN, Dzyuba IV. A model of nonlinear optical transmittance for insulator nanocomposites. Semiconductors 2011; 45(3): 295-301. DOI: 10.1134/S1063782611030109.

21. Derbov VL, Serov VV, Teper NI. Investigation of hydrogen atom radiation under the action of TI:Sapphire laser. Computer Optics 2010; 34(2): 156-161.

22. Alimenkov IV. Automodulation of one-dimensional waves based on nonlinear schredingger equation with nonlinearity cubic-quintic type. Computer Optics 2012; 36(1): 34-36.

23. Nguyen DT, Voisin C, Roussignol P, Roquelet C, Lauret JS, Cassabois G. Excitonic nonlinearities in single-wall carbon nanotubes. Physica Status Solidi (B) 2012; 249(5): 907-913. DOI:10.1002/pssb.201100064.

24. Agekyan VF, Serov AY, Filosofov NG, Vorob'ev LE, Melentyev GA, Shalygin VA, Nyk nen H, Suihkonen S. Excitonic spectra and electrical conductivity of epitaxial silicon-doped GaN layers. Physics of the Solid State 2013; 55(2): 296-300.

25. Shen YR. The principles of nonlinear optics. New York: John Willey & Sons; 1984.

26. Dzyuba VP, Kulchin YN, Amosov AV. The theory of heterogeneous dielectric nanostructures with non-typical low-threshold nonlinearity. Pacific Science Review A: Natural Science and Engineering 2015; 17(2): 41-47. DOI: 10.1016/j.psra.2015.12.005.

27. Kuznetsova YY, Remeika M, High AA, Hammack AT, Butov LV, Hanson M, Gossard AC. All-optical excitonic transistor. Optics Letters 2010; 35(10): 1587-1589. DOI:10.1364/OL.35.001587.

28. Hwang J, Pototschnig M, Lettow R, Zumofen G, Renn A, Gotzinger S, Sandoghdar V. A single-molecule optical transistor. 2009 IEEE LEOS Annual Meeting Conference Proceedings 2009: 286. DOI: 10.1109/LEOS.2009.5343277.

29. Andreakou P, Poltavtsev SV, Leonard JR, Calman EV, Remeika M, Kuznetsova YY, Butov LV, Wilkes J, Hanson M, Gossard AC. Optically controlled excitonic transistor. Applied Physics Letters 2014; 104(9): 091101. DOI: 10.1063/1.4866855.

30. Jain K. Optical transistor. Applied Physics Letters 1976, 28(12): 719. DOI: 10.1063/1.88627.